



Evaluating the Effectiveness of Red Onion Skin Extract Derivatives as Oilfield Scale Inhibitors

**Dominica Una^{a,b*}, Dulu Appah^b, Amieibibama Joseph^b
and Onyewuchi Akaranta^{a,c}**

^a World Bank-Africa Centre of Excellence for Oilfield Chemicals Research, University of Port Harcourt, Nigeria.

^b Department of Petroleum and Gas Engineering, University of Port Harcourt, Nigeria.

^c Department of Pure and Industrial Chemistry, University of Port Harcourt, Nigeria.

Authors' contributions

This work was carried out in collaboration among all authors. All authors read and approved the final manuscript.

Article Information

DOI: 10.9734/JENRR/2021/v9i330234

Editor(s):

(1) Sreekanth. K. J., Kuwait Institute for Scientific Research, Kuwait.

Reviewers:

(1) Mian Muhammad, University of Malakand, Pakistan.

(2) Mihai Todica, Babes-Bolyai University, Romania.

Complete Peer review History, details of the editor(s), Reviewers and additional Reviewers are available here: <https://www.sdiarticle5.com/review-history/80666>

Original Research Article

**Received 08 October 2021
Accepted 16 December 2021
Published 17 December 2021**

ABSTRACT

With growing awareness of the environmental impact of some conventional production chemicals and concerns about the depletion of non-renewable natural resources, increased efforts are being made to use renewable and non-toxic materials in the oilfield. In this study, a potential green scale inhibitor was developed from the skin of red onions and evaluated for calcium sulphate, calcium carbonate and barium scale inhibition. Based on the different extraction processes utilized, two products were obtained and characterized using FTIR and SEM and evaluated using a static jar test procedure. The FTIR results confirmed the bands that make up the major constituents (quercetin) and other important compounds, which supports the present study. Laboratory evaluation show that ROSE can efficiently inhibit calcium sulphate scale and barium sulphate scales with a good inhibition rate of greater than 75% at an optimum dosage. Effect of temperature and dosage on inhibition performance revealed that ROSE is stable at higher temperatures and can effectively inhibit calcium and barium sulphate scales at nearly the same rate without degradation but requires additional dosage to produce same result for calcium carbonate scale. Also, the effect of time reveals that scale inhibitor performs a continuous CaSO_4 and CaCO_3 inhibition. Not only

*Corresponding author: E-mail: dominica.una@gmail.com;

does ROSE perform excellently in the laboratory condition as a green scale inhibitor, but it also show a relatively close performance rate when compared to an existing commercial inhibitor which indicate that ROSE has a high potential for use in the oil industry.

Keywords: Calcium sulphate scale; calcium carbonate scale; barium sulphate scale; red onion skin; green scale inhibitor; scale inhibition.

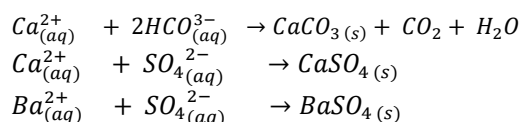
GLOSSARY

ROSE	: Red Onion Skin Extracts;
FTIR	: Fourier transform infrared spectroscopy;
NaOH	: Sodium hydroxide;
SEM	: Scanning Electron Microscope;
CaSO ₄	: Calcium sulphate;
CaCO ₃	: Calcium carbonate;
BaSO ₄	: Barium sulphate;
SrSO ₄	: strontium sulfate;
NaCl	: Sodium chloride;
CaCl ₂ •2H ₂ O	: Calcium Chloride, Dihydrate;
MgCl ₂ •6H ₂ O	: Magnesium chloride hexahydrate;
Na ₂ SO ₄	: Sodium sulfate;
BaCl ₂ •2H ₂ O	: Barium chloride, dihydrate.

1. INTRODUCTION

Scale inhibitor is a term generally used to describe a class of chemicals used to mitigate the formation or deposition of scale. Scale is an inorganic precipitation formed on metal or rock surfaces, wellbore tubulars and other wellbore equipment [1,2]. Scale inhibition can occur when one or more aspects of the crystallization process is disrupted [2,3]. Sulfate and carbonate scales have been identified as the most common inorganic scales found in oilfields worldwide [4-6] While Sulfate scales, which include calcium sulfate (CaSO₄), barium sulfate (BaSO₄) and strontium sulfate (SrSO₄) are formed due to the mixing of incompatible brines, specifically formation brine and injected seawater, carbonate scales are deposited due to change in operating conditions, such as drop in pressure in production wells [4,5,7,8]. Mineral scale

formation can be described with the following reactions [3].



To mitigate the problem of mineral scaling, chemical inhibitors are widely used. However, some of these chemical inhibitors are toxic and environmentally unsafe for application. With the increasing awareness of environmental impact caused by hazardous production chemicals, efforts have been made to utilize green scale inhibitors. Recently, green inhibitors, have raised great interest because they are biodegradable, non-toxic and do not affect environment non-bioaccumulation [9-11].

Quercetin, as shown in Fig. 1a has been discovered to have good inhibiting effect due to its high antioxidative and excellent metal chelation properties like other flavonoids [12-18]. The metal chelating property is attributed to the presence of five (5) hydroxyl groups at positions 3,3',4',5,7, and a carbonyl group at position 4 as shown in Fig. 1b [3]. Red onion skin (ROS) contains the highest concentration of "quercetin" [19,20] and other polyphenolic compounds [21,22] which can easily be extracted and used in the oil industry. However, "onion skins" are usually discarded as wastes which becomes a nuisance to the environment especially when they are disposed improperly the discovery of this active ingredient in red onion skin prompted this investigation to harness the properties of quercetin as a potential green scale inhibitor.

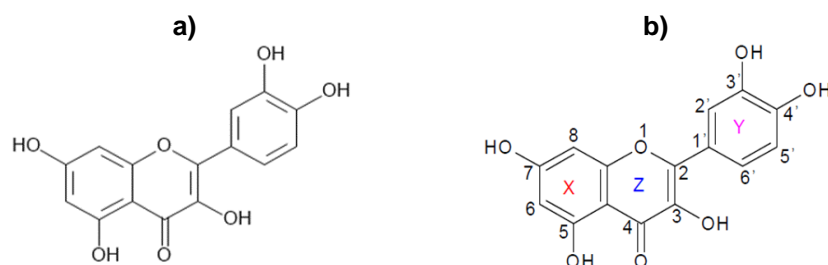


Fig. 1. (a) Structure of quercetin, (b) Functional group positions of quercetin [3]

2. MATERIALS AND METHODS

2.1 Collection and Pretreatment of ROS

Discarded onion skins from processed onions were collected from markets in Port Harcourt, Rivers State, Nigeria. They were carefully selected and thoroughly washed with distilled water to remove impurities. Thereafter, air dried at ambient temperature and pulverized into powder form using a fabricated grinder and then stored in airtight plastic containers for further use.

2.2 Extraction Process

This study adopted two extraction processes: a solvent extraction mechanism [3,23] and cold extraction process [24].

2.2.1 Solvent extraction method

Solvent extraction mechanism involves the use of a low boiling point liquid to get out extract from materials. The choice of this technique is its ability to extract up to 99.5 % of the extract from its bearing material, leaving 0.5 % as a residual [25]. In this study, Soxhlet extractor apparatus was used while acetone served as the extracting solvent.

2.2.2 Cold Extraction method

The second extraction method involved soaking clean red onion skin in 1 percent NaOH for 24 hours. After that, the soluble extracts were filtered. To separate red onion skin extract from water, a rotary evaporator was used. Thereafter, the extract was air dried for approximately 30 days to allow any remaining moisture to evaporate.

2.3 Characterization of Scale Inhibitor and Deposited Scale Crystal

Fourier transform infrared spectroscopy, FTIR (Agilent Cary 630, US in transmission mode from

4000 to 600 cm^{-1}) was used to determine the presence of various functional groups in the proposed scale inhibitors. Further investigation to assess the morphology of the scale deposition with and without inhibitor was carried out using Scanning electron microscope, SEM (HITACHI S-4800, Japan). Calcium sulphate, calcium carbonate, barium sulfate, depositions were carefully sampled at low/no inhibitor dosage.

2.4 Evaluation of the Inhibition Efficiency

To evaluate the inhibition efficiency, a static jar test was done using National Association of Corrosion Engineers (NACE) Standard TM0374-2007 procedures [26,27]. Table 1 shows the solutions prepared for evaluating the scale inhibition performance. After weighing a specific amount of scale inhibitor (20 ppm, 40 ppm, 60 ppm, 80 ppm and 100 ppm) into the Erlenmeyer flask, 50 mL of cation solution (as specified in NACE standard) was added and agitated for proper mixing, followed by another 50 mL of anion solution. The test bottle was sealed with a plastic stopper and wrapped in polyethylene film. The wrapped Erlenmeyer flasks were placed in the oven for a predetermined time at a constant temperature. The inhibitor efficiency was calculated based on the remaining Ca^{2+} and Ba^{2+} ions in solution using the following equation.

$$\text{Percentage inhibition (\%)} = \frac{m_2 - m_0}{m_1 - m_0} \times 100\%$$

where m_2 is the mass concentration of Ca^{2+} and Ba^{2+} ions after inhibitor functions, m_1 is the mass concentration of Ca^{2+} and Ba^{2+} ions in the solution of 50 mL deionized water without the addition of anions solution, m_0 is the mass concentration of Ca^{2+} and Ba^{2+} ions of the solution with no inhibitor. The test of the mass concentration of Ca^{2+} and Ba^{2+} ions also followed the method specified by the standard, TM0374-2007.

Table 1. Static jar test conditions

Scale type	Brine	Concentration (g/L)	Condition
CaSO ₄	cation	NaCl = 7.50; CaCl ₂ • 2H ₂ O = 11.10	70 °C & 90 °C
	anion	NaCl = 7.50; Na ₂ SO ₄ = 10.66	4 Hrs & 22 Hrs
CaCO ₃	cation	CaCl ₂ • 2H ₂ O = 12.15; MgCl ₂ • 6H ₂ O = 3.68; NaCl = 33.0	70 °C & 90 °C
	anion	NaHCO ₃ = 7.36; NaCl = 33.0	4 Hrs & 22 Hrs
BaSO ₄	cation	NaCl = 7.50, BaCl ₂ •2H ₂ O = 0.66	70 °C & 90 °C
	anion	NaCl = 7.50, Na ₂ SO ₄ = 0.80	4 Hrs & 22 Hrs

3. RESULTS AND DISCUSSION

3.1 Properties of ROSE and its Derivatives

Solubility of ROSE in aqueous medium and other parameters investigated are presented in Table 2. The pH measurement of the scale inhibitors, labelled ROSAC, ROS, were 8.5 and 8.0. This implies that the two products pass the criteria of a pH greater than five (>5). ROS was more soluble in water than ROSAC. This informed the decision to use ROS for further evaluation.

3.2 Characterization of Scale Inhibitor

The FTIR spectra shown in Fig. 2b was used to confirm the structure of the tested inhibitor (ROS). The peak value around 3257 cm^{-1} is attributed to the broad O-H stretching vibration for phenolic compounds. The aromatic C-H stretching vibrations are confirmed by peaks at 2918 cm^{-1} and 2851 cm^{-1} . The band at 1756 cm^{-1} is caused by the C=O stretching vibration, and the band at 1562 cm^{-1} is caused by the C=C and C=O stretching vibrations of the gamma-pyrone in ring C of the quercetin structure. The peak at 1439 cm^{-1} results from C-H asymmetric deformation vibration, while the peak at 1410 cm^{-1} results from the O-H deformation vibrations and the C-O stretching vibration. Peaks 870 cm^{-1} , 803 cm^{-1} and 784 cm^{-1} are due to the C-H out of plane deformation vibrations of the isolated aromatic C-H hydrogen atoms in the quercetin structure. The wavelength around 1071 cm^{-1} confirms the C-O-C stretching vibration. These observations agree with those of other works [28,3] and are consistent with the bonds that make up the major constituents (quercetin). The presence of quercetin and other important compounds supports the present study.

3.3 Evaluation of Scale Inhibition Performance

Fig. 3 depicts the inhibitor's inhibition performance of calcium sulfate (Fig. 3a), calcium carbonate (Fig. 3b), and barium sulfate (Fig. 4) with different inhibitor dosages at $71\text{ }^{\circ}\text{C}$. It was

generally observed that increasing the inhibitor dosage increases the inhibitor's inhibition efficiency. When the dosage reaches a critical level, the inhibition rate remains constant or slowly decreases.

In the case of calcium sulfate (Fig. 3a), the inhibitor demonstrated a good inhibition efficiency at a low dosage of 20 ppm, and the best inhibition efficiency of 70 % was obtained at a dosage of 80 ppm. The inhibition rate was low across all dosages in the calcium carbonate inhibition performance test (Fig. 3b). Based on the scope of this work, an inhibition efficiency of only 50% was obtained at the optimum dosage of 100 ppm. However, barium sulphate inhibition evaluation provided the highest inhibition efficiency of 83 % at a dosage of 80 ppm before reaching a plateau state (Fig. 4). As a result, ROS has a relatively good inhibition performance on both the calcium and barium sulfate scales. Figs. 3,4,5 (b) shows a close relationship in the performance of ROS and a commercial scale inhibitor (CSI) evaluated at the same laboratory condition.

3.4 Effects of Temperature and Time on the Inhibition Performance of the Antiscalant

3.4.1 Temperature

For inhibition property on calcium sulfate (Fig. 5a), when a dosage of 60 ppm was added, an identical inhibition rate of 65 % was obtained at $71\text{ }^{\circ}\text{C}$ and $90\text{ }^{\circ}\text{C}$. From Fig. 5b, the scale inhibition efficiency on calcium carbonate is greater than 40% with a dosage of 20 ppm at $71\text{ }^{\circ}\text{C}$ and nearly 60 ppm at $90\text{ }^{\circ}\text{C}$. This could be attributed to the fact that high temperatures facilitate the formation of calcium carbonate; as a result, an additional inhibitor dosage is required for improved efficiency. When the dosage is increased to a certain level (60 ppm), the inhibition rate at $90\text{ }^{\circ}\text{C}$ is greater than at $71\text{ }^{\circ}\text{C}$, indicating that more inhibitor adsorption occurs on the calcium carbonate crystal at higher temperatures [29].

Table 2. Properties of inhibitors

ROSE Derivatives	ID	Solubility in water	Colour	pH
ROSE Extracted with Acetone	ROSAC	Insoluble	Light Brown	8.5
ROSE Extracted with 1% NaOH in water	ROS	Soluble	Reddish Brown	8.0

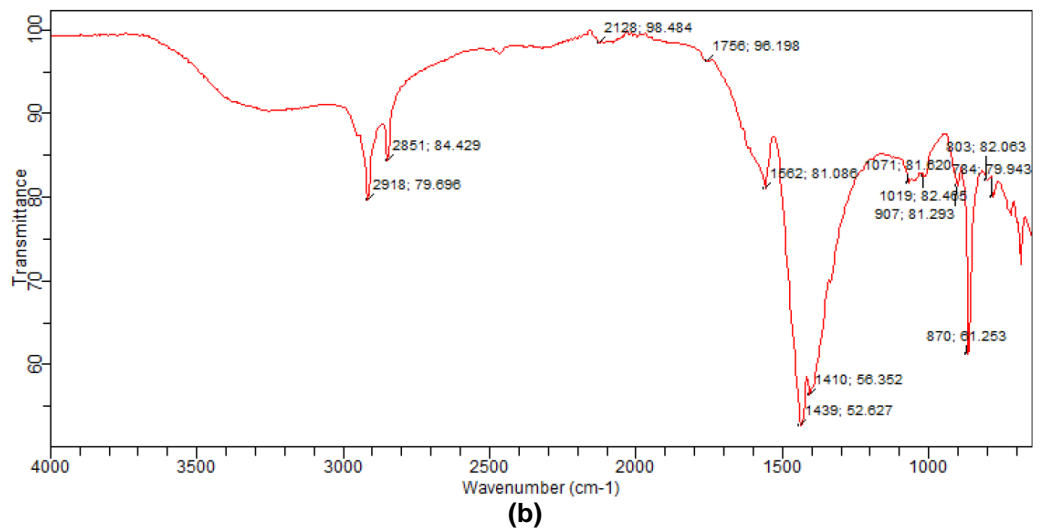
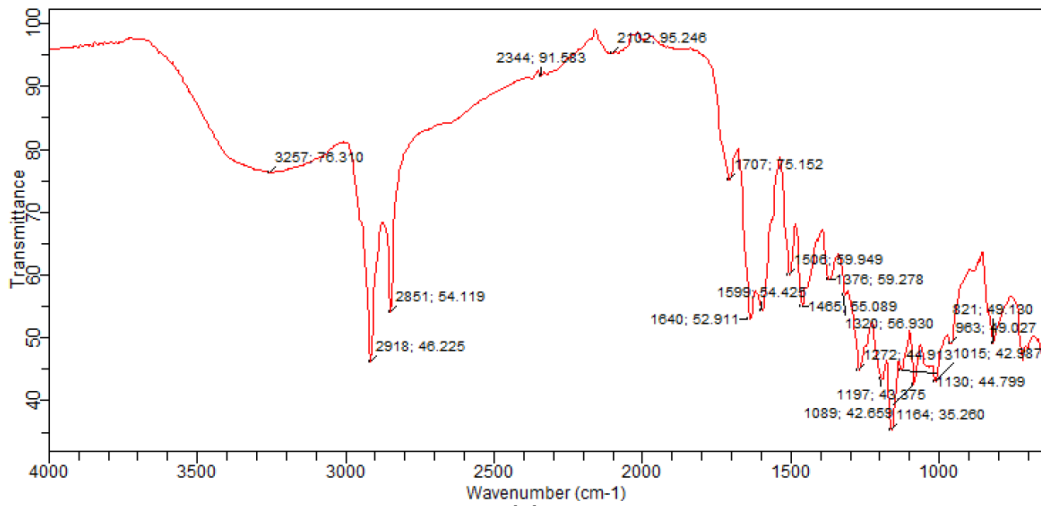


Fig. 2. FTIR spectrum of (a) ROSAC and (b) ROS

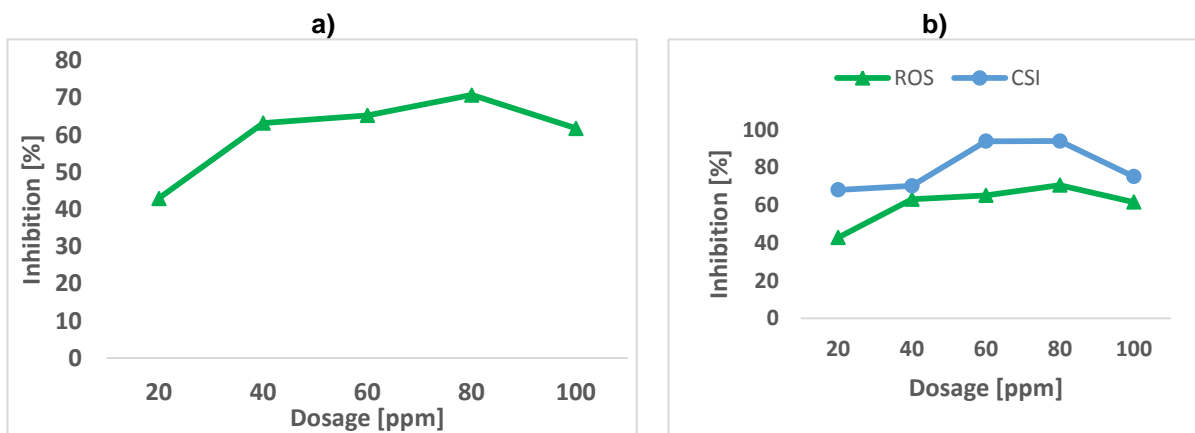


Fig. 3. a) Relation curve of dosage to inhibition efficiency of ROS on calcium sulfate scale, (b) comparison of ROS and CSI performance on calcium sulphate scale

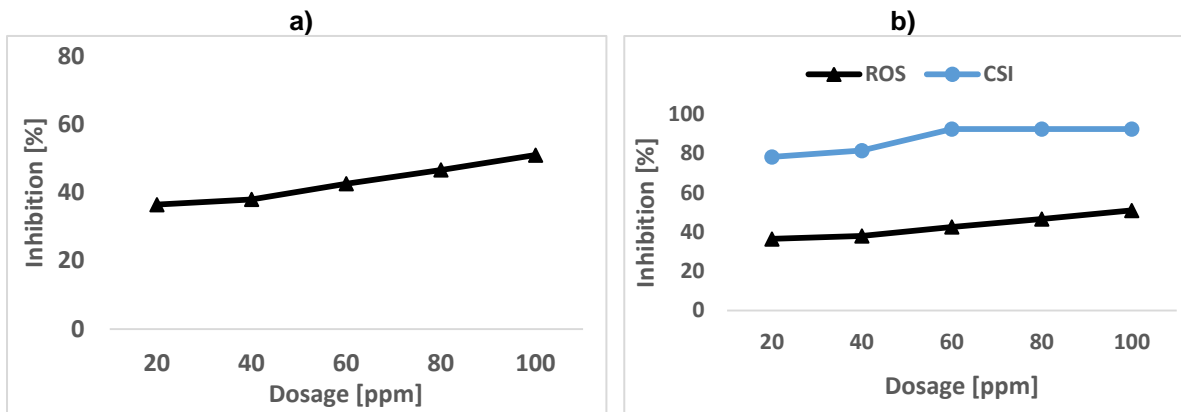


Fig. 4. a) Relation curve of dosage to inhibition efficiency of ROS on calcium carbonate scale, (b) comparison of ROS and CSI performance on calcium carbonate scale

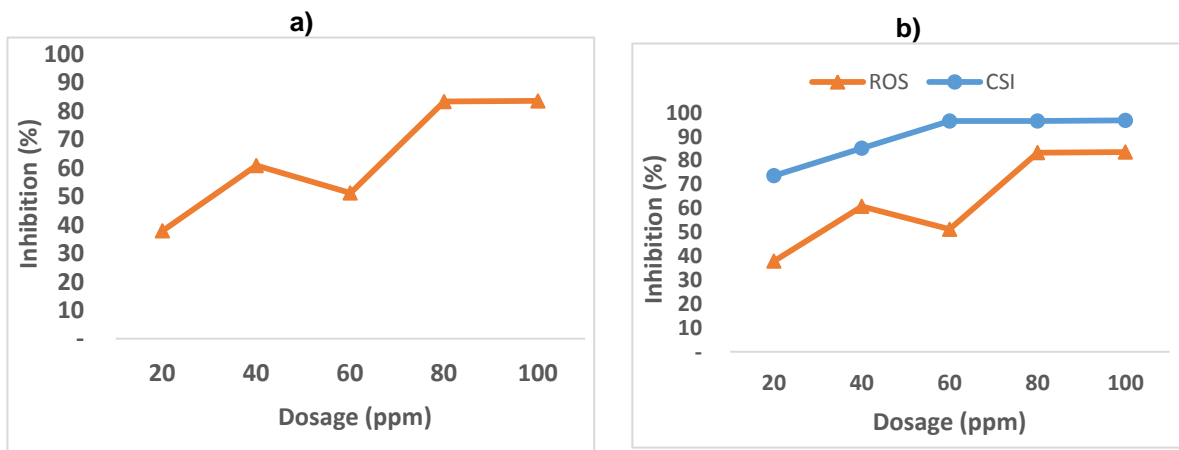


Fig. 5. a) Relation curve of dosage to inhibition efficiency of ROS on barium sulfate scale, (b) comparison of ROS and CSI performance on barium sulphate scale

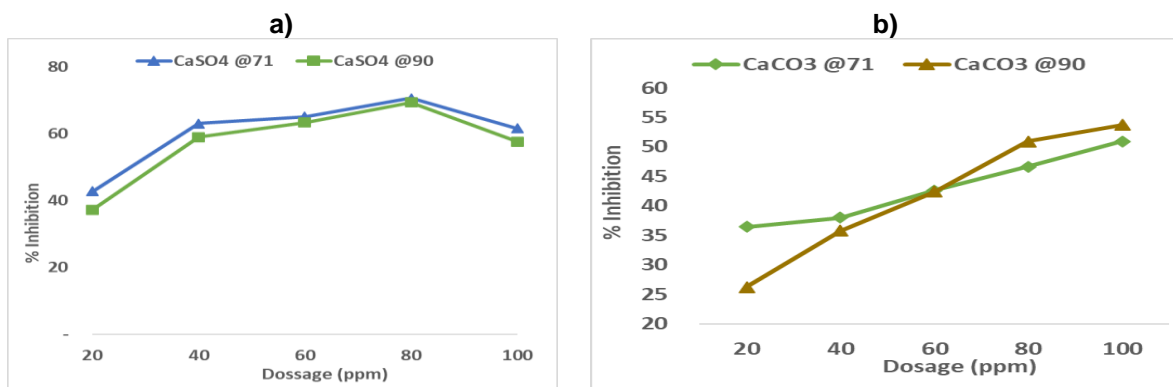


Fig. 6. Effects of temperature on the inhibition performance of ROS on (a) Calcium sulphate (b) calcium carbonate

For barium sulfate (Fig. 6), when the optimal dosage at 60 ppm was added, almost identical inhibition rate of about 60 % was obtained at both 71 °C and 90 °C. Therefore, it can be inferred that at higher temperatures, additional

inhibitor dosage is required to maintain a high inhibition rate for CaCO₃ inhibition, whereas BaSO₄ control requires no additional dosage in the scope of this work.

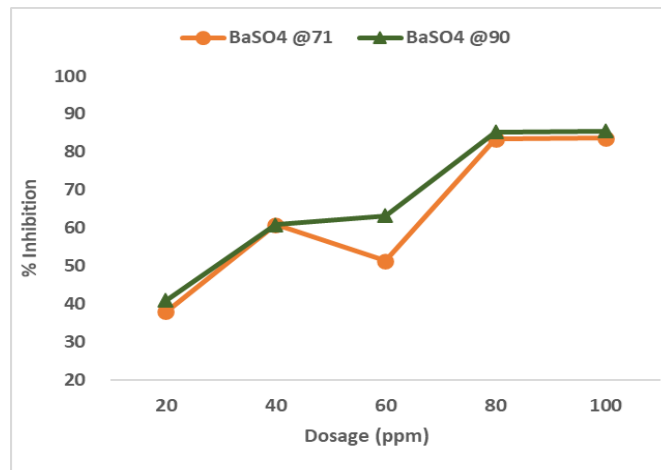


Fig. 7. Effects of temperature on the inhibition performance of ROS on barium sulphate

3.4.2 Time

Effect of inhibition time on the performance of scale inhibitor is shown in Fig. 7. For calcium sulphate deposition inhibition experiments (Fig. 7a), the scale inhibition rate increases at a higher time duration. The inhibition efficiency on calcium

carbonate is also increasing at a higher time duration (Fig. 7b). At an evaluation time of 22 hrs, CaCO₃ has an inhibition rate of 50 % which is higher when compared to 39 % obtained for 4hrs inhibition time. This indicates that the inhibitor plays a continuous CaSO₄ and CaCO₃ inhibition performance.

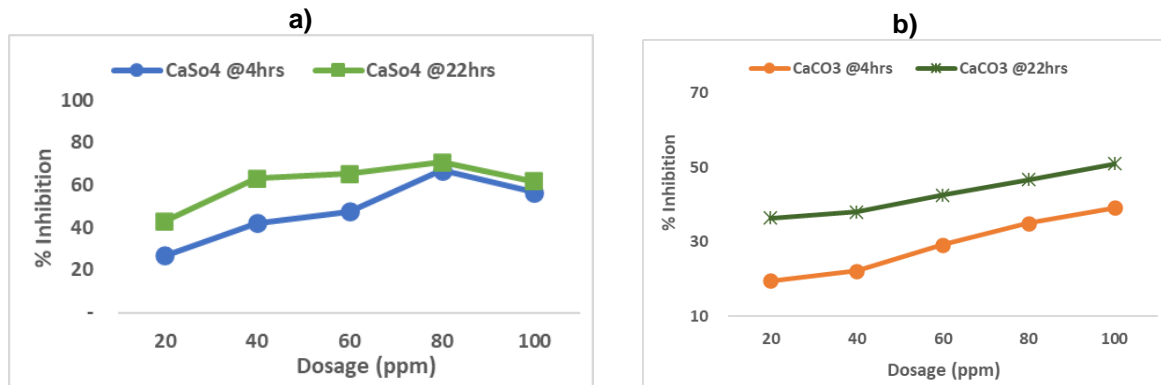


Fig. 8. Effects of time on the inhibition performance of ROS on (a) Calcium sulphate (b) calcium carbonate

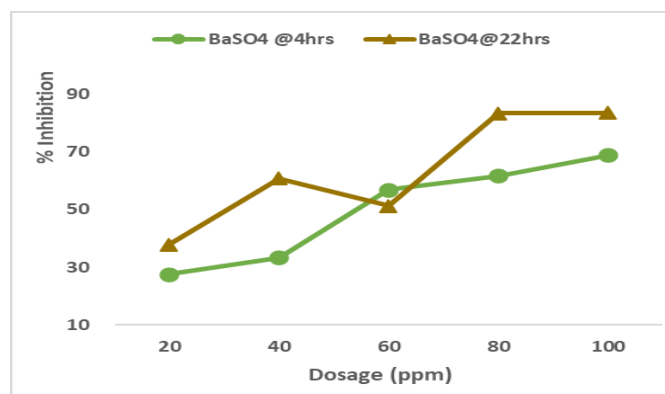


Fig. 9. Effects of time on the inhibition performance of ROS on barium sulphate

For barium sulphate deposition (Fig. 8), there was also an increase in inhibition efficiency for 22 hrs up until 60 ppm, before a sharp decrease in the inhibition rate and thereafter, a rise with increased dosage. This phenomenon suggests that a sufficient dosage for controlling barium sulfate scale deposition may be required in a long time.

3.5 SEM Analysis

SEM images of calcium sulphate, calcium carbonate, and barium sulfate, obtained from the absence and low dosage of inhibitor is shown in Figs. 9, 10, 11 respectively. When an inhibitor was added to calcium carbonate crystals, they became looser (Fig. 10c), an indication of crystal

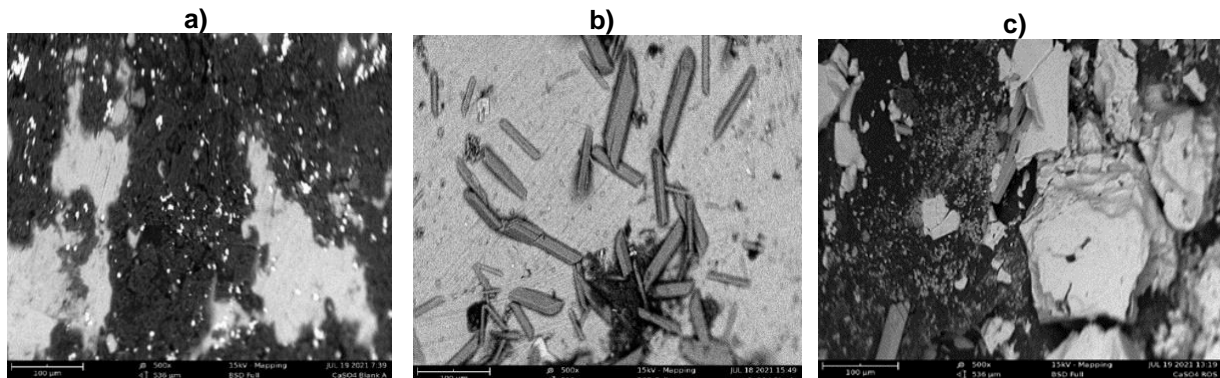


Fig. 10. SEM images of CaSO₄ without inhibitor before and after conditioning (a, b) and with inhibitor (c)

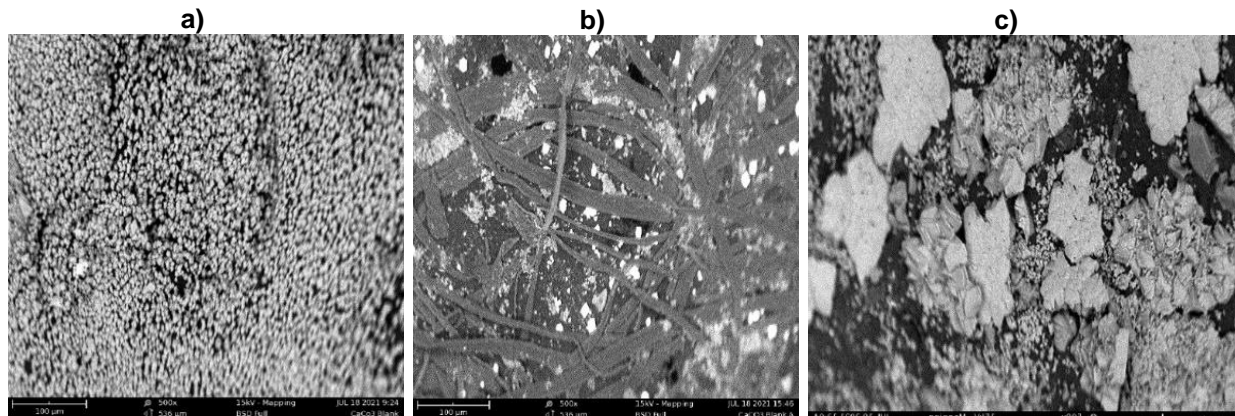


Fig. 11. SEM images of CaCO₃ without inhibitor before and after conditioning (a, b) and with inhibitor (c)

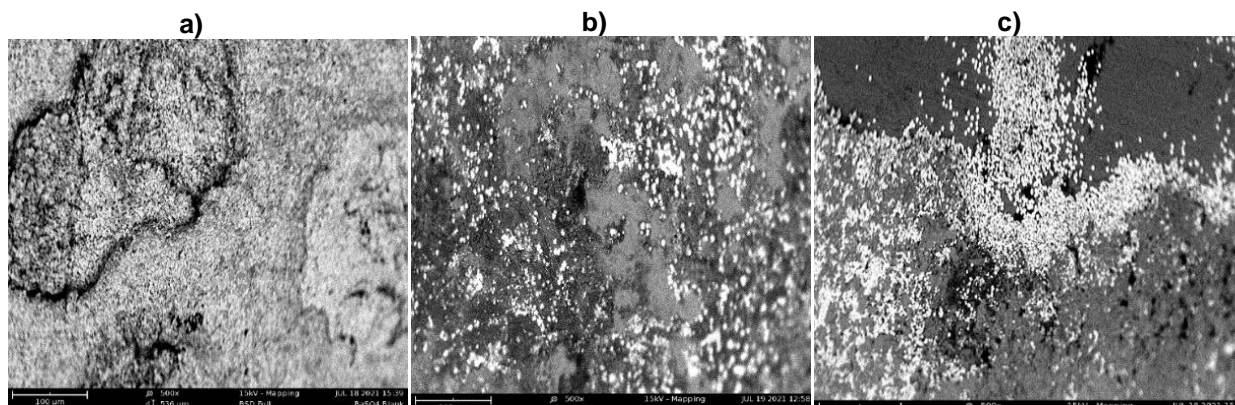


Fig. 12. SEM images of BaSO₄ without inhibitor before and after conditioning (a, b) and with inhibitor (c)

growth suppression. A similar phenomenon was observed for calcium sulfate (Fig. 9c), where the dense structure changed to loose lump. Fluid turbulence could easily disrupt the loose material, causing it to become suspended in the solution [29,30]. Also, in the presence of the inhibitor, the diameter of the calcium carbonate and calcium sulfate crystals increases, indicating that the inhibitor may have some influence on the surface phase of these scales [31]. Fig. 11 depicts a densely packed crystal of barium sulphate before conditioning and without inhibitor (Fig. 11a). Fig. 11c shows that the addition of the inhibitor resulted in loose particles. This demonstrates that the preferential growth of barium sulphate crystals was strongly inhibited.

4. CONCLUSION

1. A potential green scale inhibitor for oilfield is developed and evaluated on calcium sulfate, calcium carbonate, and barium sulfate scales. For calcium sulphate, the inhibition efficiency could be as high as 69%, and for barium sulphate, it could be as high as 85%. Calcium carbonate had a lower inhibition rate than the other scales evaluated. The highest inhibition rate of 53% was obtained at a dosage of 100 ppm.
2. The developed inhibitor has good chemical stability, high-temperature resistance, and good scale inhibition effects at low dosage.
3. Extra inhibitor is required for good inhibition of calcium carbonate deposition at higher temperatures, but it is not required for calcium sulphate and barium sulfate scale inhibition.
4. Because the diameter of calcium sulfate and calcium carbonate formed when inhibitor is present is larger than that formed at blank conditions, proper dosage is critical for calcium sulfate and calcium carbonate prevention.
5. Comparison with an existing commercial inhibitor (CSI) show that ROS has a good potential as green scale inhibitor in the oil industry.

ACKNOWLEDGEMENTS

The authors are grateful to Tetfund for the Institute Based Research (IBR) grant received which enabled the completion of this work.

COMPETING INTERESTS

Authors have declared that no competing interests exist.

REFERENCES

1. JI Al-Tammar, M Bonis, HJ Choi, Y Salim. Saudi Aramco downhole corrosion/scaling operational experience and challenges in HPHT gas condensate producers. SPE international oilfield corrosion conference and exhibition. Aberdeen, Scotland; 2014.
2. R Hosny, M Amine, M Fathy and M Ramzi M. Investigation of the Impact of Scale Inhibitors: Nonionic Surfactants for Scale Deposition Control in Oilfield. *Pet Petro Chem Eng Journal*. 2019;3(2):189.
3. Manizabayo G, Chukwu UJ, Abayeh OJ. Extraction of quercetin-rich red onion skin with acetone and chemical modification using aromatic diazonium salts. *Makara Journal of Science*. 2019;23(2):3.
4. Chen T, Neville A, Yuan M. Calcium carbonate scale formation-assessing the initial stages of precipitation and deposition. *J Pet Sci Eng*. 2005;46(3):185-194.
5. MCM Bezerra, FF Rosario, KRSA Rosa. Scale management in deep and ultradeep water fields. *Offshore Technology Conference, Brazil*; 2013.
6. R Hosny, SEM Desouky, M Ramzi, TH Abdel-Moghny, FMS El-Dars. Novel scalechem program for monitoring and enhancing dissolution of scale deposits near wellbore. *Material Science Research India*. 2007;4(2):251-261.
7. R Hosny, SEM Desouky, M Ramzi, TH Abdel-Moghny, FMS El-Dars. Estimation of the Scale Deposits Near Wellbore via Software in the Presence of Inhibitors. *Journal of Dispersion Science and Technology*. 2009;30(2):204-212.
8. MA Awan, SM Al-Khaledi. Chemical treatments practices and philosophies in oilfields. SPE international oilfield corrosion conference and exhibition, Aberdeen, Scotland; 2014.
9. Hasson D, Shemer H, Sher A. A. State of the art of friendly green scale control inhibitors: a review article. *Ind. Eng. Chem. Res*. 2011;50:7601–7607.
10. Chaussemier M, Pourmohtasham E, Gelus D, Pécoul N, Perrot H, Lédion J, Cheap-Charpentier H, Horner O. State of art of natural inhibitors of calcium carbonate scaling. *Desalination*. 2015;356:47-55.
11. Anastas PT, Warner JC. *Green Chemistry: Theory and Practice*, Oxford University Press, New York. 1998;11:13-43.

12. Aidoud R, Kahoul A, Naamoune F. Inhibition of calcium carbonate deposition on stainless steel using olive leaf extract as a green inhibitor. *Environmental Technology Journal*. 2017;38:14-22.
13. Alrawaiq NS, Abdullah A. A Review of Flavonoid Quercetin: Metabolism, Bioactivity and Antioxidant Properties. *Int. J. PharmTech Res.* 2014;6(3):933–941.
14. Dehghan G, Khoshkam Z. Chelation of Toxic Tin (II) by Quercetin: A Spectroscopic Study. *Int. Conf. Life Sci. Technol.* 2011;3:3–5.
15. Lakhanpal P, Rai DK. Quercetin: A Versatile Flavonoid. *Internet J. Med. Update.* 2007;2(2):22–37. Available:<https://doi.org/10.4314/ijmu.v2i2.39851>
16. Liu Y, Guo M. Studies on Transition Metal-Quercetin Complexes Using Electrospray Ionization Tandem Mass Spectrometry. *Molecules.* 2015;20:8583–8594. Available:<https://doi.org/10.3390/molecules20058583>
17. Symonowicz M, Kolanek M. Flavonoids and their properties to form chelate complexes. *Biotechnol. Food Sci.* 2012; 76(1):1-7.
18. Mohd FB, Razak A, Yong PK, Abdullah LC, Yee SS, Yaw TC. The effects of Varying Solvent Polarity on Extraction Yield of Orthosiphon Stamineus Leaves. *J. Appl. Sci.* 2012;12(11):1207–1210. Available:<https://doi.org/10.3923/jas.2012.1207.1210>
19. Horbowicz M. Method of quercetin extraction from dry scales of onion. *Veget. Crops Res. Bull.* 2002;57:119-124.
20. Sayed HS, Hassan NMM, El MHA. The Effect of Using Onion Skin Powder as a Source of Dietary Fiber and Antioxidants on Properties of Dried and Fried Noodles. *Current Sci. J.* 2014;3(4):468–475.
21. Ifesan BOT. Chemical Composition of Onion Peel (*Allium cepa*) and its Ability to Serve as a Preservative in Cooked Beef. *Int. J. Sci. Res. Methodol.* 2017;7(4):1-10.
22. MO Bello, IO Olabanji, M Abdul-Hammed and TD Okunade. Characterization of domestic onion wastes and bulb (*Allium cepa* L.): fatty acids and metal contents. *Int. Food Res. J.* 2013;20(5):2153– 2158.
23. Akaho AA, Chukwu UJ, Akaranta O. Cu (II)-Red Onion Skin Extract-Azo metal Complex - A Potential for Oilfield. *Chemical Science International Journal.* 2019;24-56.
24. Itodo SE, Oyero, EU Umeh, Ben A, Etubi MD. Phytochemical Properties and Staining Ability of Red Onion S (*Allium cepa*) Extract on Histological Sections. *J Cytol Histol.* 2014;5:275. DOI: 10.4172/2157-7099.1000275
25. Dike HN, Dosunmu A, Akaranta O, Kinigoma B. Effect of Cashew Nut Shell Liquid Esters on KCL/Polymer/Glycol Drilling Fluid Flow Property. *International Journal of Technical & Scientific Research Engineering.* 2019;2:2581-9259.
26. NACE Standard TM0197-2010, Item No. 21228, Laboratory Screening Test to Determine the Ability of Scale Inhibitors to Prevent the Precipitation of Barium Sulfate or Strontium Sulfate, or Both, from Solution (for Oil and Gas Production Systems).
27. NACE Standard TM0374-2007 (formerly TM0374-2001) Item No. 21208, Laboratory Screening Tests to Determine the Ability of Scale Inhibitors to Prevent the Precipitation of Calcium Sulfate and Calcium Carbonate from Solution (for Oil and Gas Production Systems).
28. Heneczkowski M, Kopacz M, Nowak D, Kuźniar A. Infrared spectrum analysis of some flavonoids. *Acta Pol Pharm.* 2001;58:415-20.
29. Luo H, Chen D, Yang X, Zhao X, Feng H, Li M, Wang J. Synthesis and performance of a polymeric scale inhibitor for oilfield application. *J Petrol Explor Prod Technol.* 2015;5:177–187.
30. Shen ZH, Li JS, Xu K, Ding LL, Ren HQ. The effect of synthesized hydrolyzed polymaleic anhydride (HPMA) on the crystal of calcium carbonate. *Desalination.* 2012;284:238–244.
31. Mavredaki E, Neville A, Sorbie KS. Initial Stages of Barium Sulfate Formation at Surfaces in the Presence of Inhibitors. *Cryst Growth Des.* 2011;11:4751–4758.

© 2021 Una et al.; This is an Open Access article distributed under the terms of the Creative Commons Attribution License (<http://creativecommons.org/licenses/by/4.0>), which permits unrestricted use, distribution, and reproduction in any medium, provided the original work is properly cited.

Peer-review history:
 The peer review history for this paper can be accessed here:
<https://www.sdiarticle5.com/review-history/80666>